Dynamics of Class 1 Tensegrity Systems Including Cable Mass

Raman Goyal[1] and Robert E. Skelton[2]

[1]Graduate Student, Dept. of Aerospace Engineering, Texas A&M Univ., TX, USA. E-mail: ramaniitrgoyal92@tamu.edu
[2]TEES Distinguished Research Professor, Dept. of Aerospace Engineering, Texas A&M Univ., TX, USA. E-mail: bobskelton@tamu.edu

ABSTRACT

Previous dynamic models of tensegrity systems either used finite element methods, which do not preserve correct rotational dynamics, or exact rotational dynamics with massless cables. This paper allows any specified discretization of the cable masses, while preserving the exact rigid bar dynamics. The model has a matrix second order form. This model is non-minimal (6 DOF for each bar instead of 5) in order to preserve the minimal complexity of the model. This is important since dynamic models can be solved more accurately in computer simulations if the mathematical structure of the model is simplified and exploited during the computations. This matrix representation of tensegrity dynamics has the simplest structure, yielding the most accurate simulations, we believe. The second simplification of these nonlinear dynamic equations is a characterization of the control variable as the force density in each cable. The actual control might be the rest length of the cable, but it is a simple yet nonlinear change of variable to convert to force density control variables, and this leads to the advantage of linear equations in the control variable, even though the model is very nonlinear in the state. This model allows skins and surfaces to be modeled on the tensegrity dynamics, a large improvement over previous nonlinear dynamic models of tensegrity.

INTRODUCTION

The field of Multi-Body Dynamics includes rigid and elastic bodies connected in arbitrary ways. *Tensegrity* systems is a subset of this class of problems that fits many problems, but this subset is not as general as the broad definition of Multi-Body dynamics. In tensegrity, we define a rod as a rigid body with negligible inertia about the longitudinal axis of the rod, and we allow rod-to-rod and rod to elastic tension members to be connected along the centerline and at the end of the rods. Mathematically this corresponds to connections with frictionless ball joints (Lalvani 1996). Skelton (Skelton and de Oliveira 2009) describes tensegrity as a network of axially loaded prestressable members, where class 1 tensegrity allows only one rod to touch any node, and a class k tensegrity allows up to k rods to join at a node. The topology of rod/string networks can be optimized subject to certain constraints and performance objectives. For example, the five fundamental questions in engineering mechanics might be considered as: i) What is the minimal mass material topology to take compressive loads?, ii) torsional loads?, iii) simply-supported bending loads?, iv) cantilevered bending loads?, v) tension loads? Tensegrity structures provide the answer to such questions. These elementary results guide the way toward the choice of elementary building blocks to build more complex structures (Skelton and de Oliveira 2010). Tensegrity architecture appears in many biological systems, such as the bone and muscle networks, fibrous structural components in living cells and the molecular structure of spider fiber (Skelton and de Oliveira 2010; Ingber 1998). Tensegrity concepts are also providing solutions to many structural problems, such as artificial gravity space habitats (Skelton and Longman 2014;

Goyal et al. 2017), civil engineering bridges (Carpentieri et al. 2015; Nagase and Skelton 2014; Carpentieri and Skelton 2016; Carpentieri et al. 2016) and impact structures (SunSpiral et al. 2013; Rimoli 2016). In addition to those dynamic studies, minimal mass properties of those structural configurations are also analyzed (Skelton and de Oliveira 2010; Nagase and Skelton 2014; Skelton et al. 2016).

At a fundamental level, modeling these structures, as well as their dynamics, is straightforward since it relies simply on the dynamics of rigid bars. A key aspect in working with these systems, however, is scalability. A rigorous and scalable approach to describing these structures is highly desirable. The derivation contained herein allows for modeling of tensegrity systems with flexible massive string members and elastic "skins".

Class 1 tensegrity systems (Skelton and de Oliveira 2009) have been described as a network of axially-loaded members with disjointed compressive members; strings only in tension, bars (rods) only in compression. The absence of bending in *individual* elements still allows the *overall* system to bend. The dynamics of such systems have been described in (Skelton 2005), where the tension members are massless. Obviously there are many applications, such as cable-stayed bridges, in which the mass of the cables are as important as the mass of the rods. Furthermore, applications exist in which a membrane covering the surface of the structure is required. This paper therefore makes three contributions to the theory and mathematical modeling of tensegrity systems:

1. String mass is added to the strings
2. Elastic skin can be added to the structure
3. The total system is modeled in matrix form, without the use of any transcendental functions

The absence of trigonometric functions leads to improved accuracy and efficiency of the simulation and/or control design.

The importance of this work will be the creation of dynamical systems which use control of the internal tension members to achieve dynamic responses that can achieve a larger variety of performance objectives than possible with existing materials and control actuation methods. At a smaller scale, this work can create a new kind of material that can follow shape control commands.

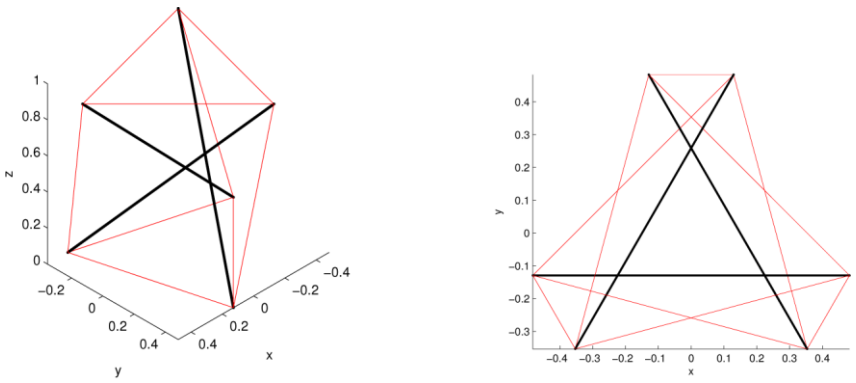

(a) Isometric view (b) Top view

FIG. 1: Tensegrity triangular prism structure.

NON-MINIMAL DYNAMICAL MODEL

The non-minimal tensegrity model introduced in (Skelton 2005) and extended to bar-to-bar

joints in (Cheong and Skelton 2015) serves as the basis of the novel extended model developed here. This non-minimal model was selected as the starting point because it best represents the state of the art of tensegrity modeling. It directly describes tensegrity system dynamics in terms of bar endpoint (node) positions – a non-minimal realization that is desirable for shape-driven applications. Additionally, it fully describes the nonlinear dynamics of tensegrity systems in a compact way that is computationally efficient—a second order matrix differential equation that does not require the use of any transcendental functions. This model is given as follows:

$$\ddot{N}M + NK = W \tag{1}$$

where

$$M = \frac{1}{12} C_b^\top \hat{m}_b C_b + C_r^\top \hat{m}_b C_r$$

$$K = C_s^\top \hat{\gamma} C_s - C_b^\top \hat{\lambda} C_b$$

$$\hat{\lambda} = -\frac{1}{12} \hat{m}_b \hat{l}^{-2} \left\lfloor C_b \dot{N}^\top C_b^\top \right\rfloor - \frac{1}{2} \hat{l}^{-2} \left\lfloor C_b N^\top F C_b^\top \right\rfloor.$$

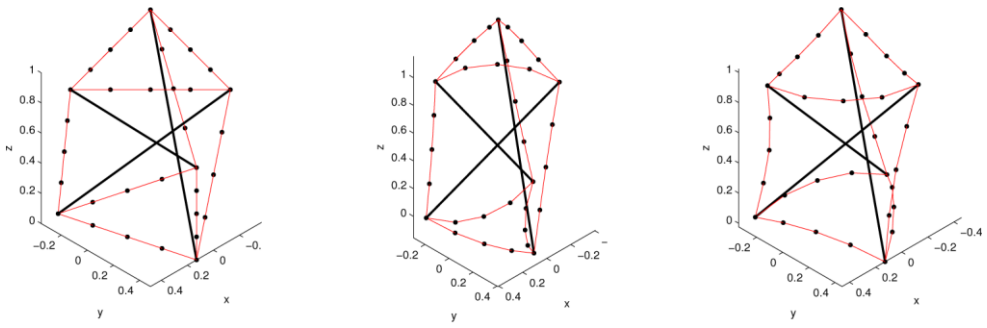

(a) t = 0 sec (b) t = 0.24 sec (c) t = 0.39 sec

FIG. 2: Simulation time-lapse of prism structure using string-to-string connections to model string mass.

A full derivation of this model can be found in (Cheong and Skelton 2015) but terms are defined here. N is a matrix describing all node positions, M is analogous to a time-invariant mass matrix, K is a matrix that is a function of tension in strings and compression in bars, W is a matrix describing external forces acting on all nodes, C_b is the bar connectivity matrix describing how bar members are defined in terms of node positions, $\hat{m}_b$ is a diagonal matrix of all bar masses, C_r is a connectivity matrix used to determine center of mass positions for each bar member, C_s is the string connectivity matrix describing how string members are defined in terms of node positions, $\hat{\gamma}$ is a diagonal matrix of string force densities (tension divided by length), $\hat{\lambda}$ is a diagonal matrix of bar force densities, $\hat{l}$ is a diagonal matrix of bar lengths, and F is a force matrix describing the sum of external and internal forces acting on bar members and is expressed as

$$F = W - NC_s^\top \hat{\gamma} C_s.$$

The bar and string connectivity matrices are defined such that bar and string member matrices, describing the lengths and orientations of all structural members, can be written as

$$B = NC_b^\top$$

$$S = NC_s^\top.$$

Similarly, R, a matrix describing the center of mass positions of each bar member, can be expressed with

$$R = NC_r^\top.$$

These connectivity matrix definitions are worth emphasizing here because they serve as the basis of additional connectivity matrices introduced in this work.

STRING-TO-STRING POINT MASS NODES

The above equations of dynamics does not account for string mass. It is desirable to develop a method of modeling string masses. This is achieved by adding nodes that connect to no bars (string-to-string nodes) that have some associated point mass. In this way, as a simple example, a string member can be modeled as two connected strings with a point mass at the point of connection. In this simple case, the mass of the string would be modeled as being at the center of the original string member. Additional granularity can be modeled by subdividing the original string into n connected string members with $n - 1$ connection point masses.

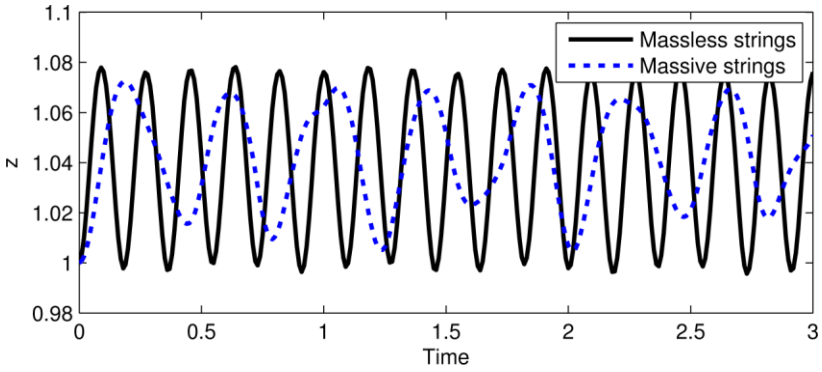

FIG. 3: Node 1 z-coordinate time history for tensegrity prism with massless and massive strings.

The process of modeling string masses as described begins with denoting two types of nodes: bar nodes, which are the end points of bars, and string nodes, which are the locations of string-to-string joints that have a point mass associated with them. The full node matrix can consequently be split as follows: $N = [N_b \quad N_s]$. Here, N_b is a $3 \times 2\beta$ matrix in which each column is the position of a bar node n_b, and N_s is a $3 \times \sigma$ matrix in which each column is the position of a string node n_s where, β and σ represent the number of bars and number of string nodes respectively. Note that the bar and string nodes can be extracted from the node matrix N with the definition of two new "node specification" connectivity matrices, $C_{nb}^\top$ and $C_{ns}^\top$:

$$N_b = N\begin{bmatrix} I_{2\beta} \\ 0 \end{bmatrix} = NC_{nb}^\top$$

$$N_s = N\begin{bmatrix} 0 \\ I_\sigma \end{bmatrix} = NC_{ns}^\top$$

where I is an identity matrix.

The center of mass matrix R can similarly be broken into two components: R_b, which describes the center of mass locations for each bar member, and R_s, which describes the location of each string point mass. These center of mass matrices can also be expressed in terms of the

defined node specification connectivity matrices.

$$R_b = N_b C_r^\top = N C_{nb}^\top C_r^\top$$

$$R_s = N_s = N C_{ns}^\top.$$

Similarly, the expression for the bar member matrix B can be rewritten in terms of the full node matrix and bar node specification connectivity matrix. Note that the bar connectivity matrix remains unchanged from its original definition.

$$B = N_b C_b^\top = N C_{nb}^\top C_b^\top.$$

As new string members are being added to the model, the original string connectivity matrix C_s must be redefined. Here, C_s is separated into two parts–the first, C_{sb}, describing bar-to-string joints and the second, C_{ss}, describing string-to-string joints.

$$S = N C_s^\top = \begin{bmatrix} N_b & N_s \end{bmatrix} \begin{bmatrix} C_{sb}^\top \\ C_{ss}^\top \end{bmatrix}.$$

The original expression for the force matrix F remains unchanged, though it is now describing the sum of forces acting on bar nodes, F_b, as well as string nodes, F_s.

$$F = \begin{bmatrix} F_b & F_s \end{bmatrix} = W - N C_s^\top \hat{\gamma} C_s. \tag{2}$$

Modeling the dynamics of the newly defined string nodes requires their translational dynamics. Because the string nodes are simply point masses, expressing their translational dynamics from vector to matrix form is straightforward:

$$m_s \ddot{r}_s = f_s \rightarrow \ddot{R}_s \hat{m}_s = F_s \tag{3}$$

where m_s is the mass of a string point node, r_s is the position of that node and f_s is the total external force on that node.

The dynamics of the bar members (developed in the derivation of Equation 1 (Cheong and Skelton 2015)) must be slightly modified to reflect the subdivision of the force matrix F.

$$\ddot{R}_b \hat{m}_b = 2 F_b C_r^\top \tag{4}$$

$$\frac{1}{12} \ddot{B} \hat{m}_b = \frac{1}{2} F_b C_b^\top + B \hat{\lambda}. \tag{5}$$

Equations 3, 4, and 5 can be written in a matrix form as follows:

$$\begin{bmatrix} \ddot{B} & \ddot{R}_b & \ddot{R}_s \end{bmatrix} \begin{bmatrix} \frac{1}{12}\hat{m}_b & 0 & 0 \\ 0 & \hat{m}_b & 0 \\ 0 & 0 & \hat{m}_s \end{bmatrix} + \begin{bmatrix} B & R_b & R_s \end{bmatrix} \begin{bmatrix} -\hat{\lambda} & 0 & 0 \\ 0 & 0 & 0 \\ 0 & 0 & 0 \end{bmatrix} = \begin{bmatrix} \frac{1}{12} F_b C_b^\top & 2 F_b C_r^\top & F_s \end{bmatrix}.$$

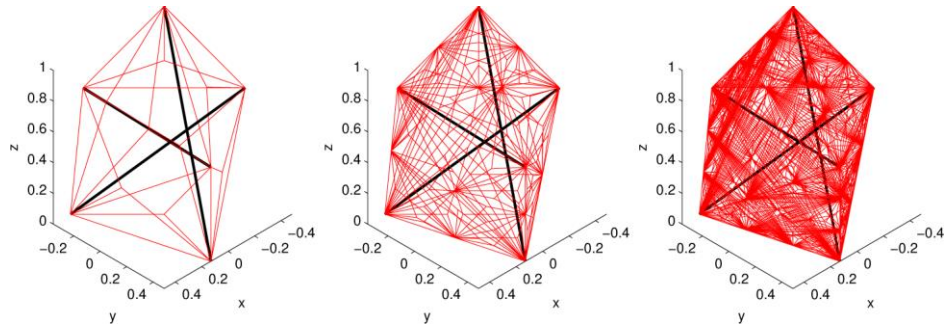

FIG. 4: Prism structure with elastic skin modeled with varying complexity.

Because the force matrix F has been defined as $F = \begin{bmatrix} F_b & F_s \end{bmatrix}$, the force term can be rewritten in terms of F.

$$\begin{bmatrix} \ddot{B} & \ddot{R}_b & \ddot{R}_s \end{bmatrix} \begin{bmatrix} \frac{1}{12}\hat{m}_b & 0 & 0 \\ 0 & \hat{m}_b & 0 \\ 0 & 0 & \hat{m}_s \end{bmatrix} + \begin{bmatrix} B & R_b & R_s \end{bmatrix} \begin{bmatrix} -\hat{\lambda} & 0 & 0 \\ 0 & 0 & 0 \\ 0 & 0 & 0 \end{bmatrix} = F \begin{bmatrix} \frac{1}{2}C_b^\top & 2C_r^\top & 0 \\ 0 & 0 & I \end{bmatrix}. \quad (6)$$

Recognizing that $\begin{bmatrix} \frac{1}{2}C_b^\top & 2C_r^\top \end{bmatrix}^{-1} = \begin{bmatrix} C_b^\top & C_r^\top \end{bmatrix}^\top$, it can be shown that

$$\begin{bmatrix} \frac{1}{2}C_b^\top & 2C_r^\top & 0 \\ 0 & 0 & I \end{bmatrix}^{-1} = \begin{bmatrix} C_b & 0 \\ C_r & 0 \\ 0 & I \end{bmatrix}.$$

The previous expression allows Equation 6 to be rewritten as follows:

$$\begin{bmatrix} \ddot{B} & \ddot{R}_b & \ddot{R}_s \end{bmatrix} \begin{bmatrix} \frac{1}{12}\hat{m}_b & 0 & 0 \\ 0 & \hat{m}_b & 0 \\ 0 & 0 & \hat{m}_s \end{bmatrix} \begin{bmatrix} C_b & 0 \\ C_r & 0 \\ 0 & I \end{bmatrix} + \begin{bmatrix} B & R_b & R_s \end{bmatrix} \begin{bmatrix} -\hat{\lambda} & 0 & 0 \\ 0 & 0 & 0 \\ 0 & 0 & 0 \end{bmatrix} \begin{bmatrix} C_b & 0 \\ C_r & 0 \\ 0 & I \end{bmatrix} = F.$$

As previously defined B, R_b, and R_s in terms of N and connectivity matrices as

$$\begin{bmatrix} B & R_b & R_s \end{bmatrix} = N \begin{bmatrix} C_{nb}^\top C_b^\top & C_{nb}^\top C_r^\top & C_{ns}^\top \end{bmatrix}.$$

The above expression can be substituted into the matrix expression for the full system dynamics.

$$\ddot{N} \begin{bmatrix} C_{nb}^\top C_b^\top & C_{nb}^\top C_r^\top & C_{ns}^\top \end{bmatrix} \begin{bmatrix} \frac{1}{12}\hat{m}_b & 0 & 0 \\ 0 & \hat{m}_b & 0 \\ 0 & 0 & \hat{m}_s \end{bmatrix} \begin{bmatrix} C_b & 0 \\ C_r & 0 \\ 0 & I \end{bmatrix} + \ddot{N} \begin{bmatrix} C_{nb}^\top C_b^\top & C_{nb}^\top C_r^\top & C_{ns}^\top \end{bmatrix}$$

$$\begin{bmatrix} -\hat{\lambda} & 0 & 0 \\ 0 & 0 & 0 \\ 0 & 0 & 0 \end{bmatrix} \begin{bmatrix} C_b & 0 \\ C_r & 0 \\ 0 & I \end{bmatrix} = F.$$

Multiplying this out, substituting Equation 2 for F, and rearranging yields the following expression for the full system dynamics:

$$\ddot{N} \begin{bmatrix} \frac{1}{12} C_{nb}^\top C_b^\top \hat{m}_b C_b + C_{nb}^\top C_r^\top \hat{m}_b C_b & C_{ns}^\top \hat{m}_s \end{bmatrix} + N \begin{bmatrix} C_s^\top \hat{\gamma} C_{sb} - C_{nb}^\top C_b^\top \hat{\lambda} C_b & C_s^\top \hat{\gamma} C_{ss} \end{bmatrix} = W.$$

Following the example set in Equation 1, a compact matrix form for the full system dynamics including string masses can be obtained with the following definitions of M_s and K_s.

$$\ddot{N} M_s + N K_s = W \quad (7)$$

$$M_s = \begin{bmatrix} C_{nb}^\top \left(\frac{1}{12} C_b^\top \hat{m}_b C_b + C_r^\top \hat{m}_b C_r \right) & C_{ns}^\top \hat{m}_s \end{bmatrix} \tag{8}$$

$$K_s = \begin{bmatrix} C_s^\top \hat{\gamma} C_{sb} - C_{nb}^\top C_b^\top \hat{\lambda} C_b & C_s^\top \hat{\gamma} C_{ss} \end{bmatrix}. \tag{9}$$

RESULTS AND EXAMPLES

Example 1

To illustrate handling of string-to-string connections, example structures are defined herein. Initial conditions are specified, and corresponding simulation results are given. The first structure here is a traditional tensegrity triangular prism shown in Figure 1. This structure has 3 bars (shown in black) and 9 strings (shown in red). In the absence of external forces, this structure has a known equilibrium solution — if the top and bottom string members have force density value $\gamma_t = \gamma_b$, the vertical string members must have force density value $\gamma_v = \sqrt{3}\gamma_t$ (Skelton and de Oliveira 2009).

To demonstrate modeling of flexible string members with mass, each string member in prism structure is subdivided into, in this case, three point masses and four string segments. The resulting structure is shown in Figure 2a. For demonstration purposes, bar masses are specified as 1 kg, and point masses are specified as 0.01 kg. Initial force density values are deliberately specified as $\gamma_t = \gamma_b = 17.3205$ N/m and $\gamma_v = 9$ N/m to induce motion. Bar lengths, based on specified initial node positions, are 1.3903 m long and all string members are given stiffness values of 100 N/m.

A three-figure time-lapse illustrating the motion of the flexible massive strings in the resulting dynamic simulation is given in Figure 2. To illustrate the effects of string mass, a time history of the z-coordinate of Node 1, initially at (0.4830, −0.1294, 1), is given in Figure 3 with and without string mass modeled. As can be seen, inclusion of string mass significantly changes the motion of the node.

Example 2

This example demonstrates how an elastic skin membrane can be modeled as a mesh of string-to-string joints, and how the addition of skin membranes to a given structure can increase its stiffness. The developed dynamical model, by including string-to-string connections, allows generation of interconnected elastic string meshes that can be attached to bar members. An elastic skin membrane can be modeled as a mesh of interconnected string members with any number of topologies. Figure 4 shows a prism structure with skin added using one example topology generation method that allows parameterizable complexity. In this case, a node is placed at the center of each external polygon of the structure, and string members are generated that connect the node to the vertices of its parent panel. This can be done recursively for *n* iterations.

To illustrate how the inclusion of skin affects dynamical response of a structure, skin panels are added to the top and bottom surfaces of a prism structure (illustrated in Figure 5). Simulations are performed for the structure with and without the skin panels with identical initial conditions for the original string members to allow comparison. Comparing the node 1 z-coordinate time histories for the structure with and without the skin membranes shows that displacement is reduced with inclusion of the skin.

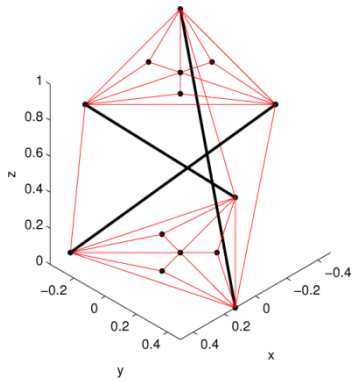

FIG. 5: Prism structure with elastic skin added to top and bottom panels. Complexity *n* = 2

CONCLUSIONS

A number of conclusions can be made based on the presented work. First, the ability to include string-to-string joints in the developed dynamical model allows for modeling and simulation of massive string members, elastic skin membranes, and Class 0 string meshes. Modeling and simulation results for each of these cases have been presented. Second, it is evident that accounting for string mass in simulation changes the dynamical response of a given structure. Simulation results show that even structures with low total string mass relative to bar mass exhibit this discrepancy. Finally, it has been shown that the inclusion of elastic skin membranes on a structure can increase the stiffness of the structure.

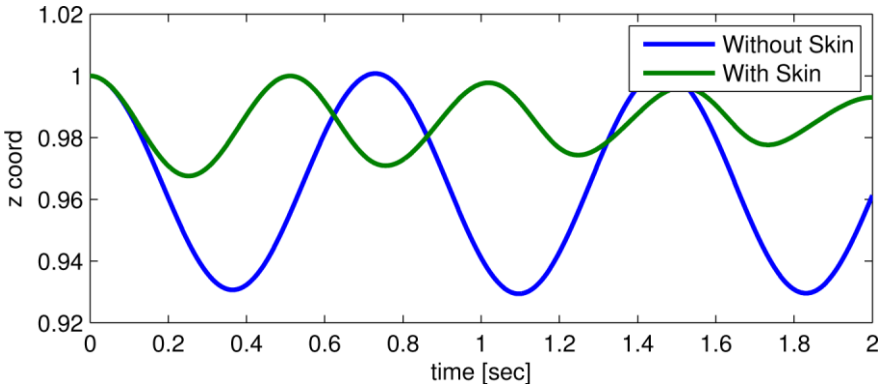

FIG. 6: Stiffness comparison of prism structure with and without skin panels shown in Figure 5

ACKNOWLEDGEMENT

The author would like to thank Mr. James V Henrickson for assisting in writing the code and in generating the examples.

REFERENCES

Carpentieri, G. and Skelton, R. E. (2016). “On the minimal mass design of composite membranes.” *Composites Part B: Engineering*, 115(3-4), 244–256.

Carpentieri, G., Skelton, R. E., and Fraternali, F. (2015). “Minimum mass and optimal complexity of planar tensegrity bridges.” *International Journal of Space Structures*, 30(3-4), 221–243.

Carpentieri, G., Skelton, R. E., and Fraternali, F. (2016). "A minimal mass deployable structure for solar energy harvesting on water canals." *Structural and Multidisciplinary Optimization*, 55(2), 449–458.

Cheong, J. and Skelton, R. E. (2015). "Nonminimal dynamics of general class k tensegrity systems." *International Journal of Structural Stability and Dynamics*, 15(2), 1450042 (22 pages).

Goyal, R., Bryant, T., Majji, M., Skelton, R., and Longman, A. (2017). "Design and control of growth adaptable artificial gravity space habitats." *AIAA SPACE and Astronautics Forum and Exposition, Orlando, FL.*, 5141 (15 Pages).

Ingber, D. E. (1998). "The architecture of life." *Scientific America*, 278(1), 48–57.

Lalvani, H. (1996). "Origins of tensegrity: Views of emmerich, fuller and snelson." *International Journal of Space Structures*, 11(1-2), 27.

Nagase, K. and Skelton, R. E. (2014). "Double-helix tensegrity structures." *AIAA Journal*, 53(4), 847–862.

Rimoli, J. J. (2016). "On the impact tolerance of tensegrity-based planetary lan-ders." *57th AIAA/ASCE/AHS/ASC Structures, Structural Dynamics, and Materials Conference, AIAA SciTech Forum*, 1511 (8 Pages).

Skelton, R. (2005). "Dynamics and control of tensegrity systems." *IUTAM Symposium on Vibration Control of Nonlinear Mechanisms and Structures*, Vol. 130, Springer, 309–318.

Skelton, R. and de Oliveira, M. (2009). *Tensegrity Systems*. Springer US.

Skelton, R. and Longman, A. (2014). "Growth capable tensegrity structures as an enabler of space colonization." *AIAA Space 2014 Conference and Exposition, San Diego, CA*, 4370 (16 Pages).

Skelton, R. E. and de Oliveira, M. C. (2010). "Optimal complexity of deployable compressive structures." *Journal of the Franklin Institute*, 347(1), 228–256.

Skelton, R. E., Montuori, R., and Pecoraro, V. (2016). "Globally stable minimal mass compressive tensegrity structures." *Composite Structures*, 141, 346–354.

SunSpiral, V., Gorospe, G., Bruce, J., Iscen, A., Korbel, G., Milam, S., Agogino, A., and Atkinson, D. (2013). "Tensegrity based probes for planetary exploration: Entry, descent and landing (edl) and surface mobility analysis." *International Journal of Planetary Probes*, 7 (13 Pages).